

## Degenerate routes to chaos

Jason A. C. Gallas

*Laboratory for Plasma Research, University of Maryland, College Park, Maryland 20742-3511;**Höchstleistungsrechenzentrum, Forschungszentrum Jülich, D-52425 Jülich, Germany;**and Laboratório de Óptica Quântica, Universidade Federal de Santa Catarina, 88040-900 Florianópolis, Santa Catarina, Brazil*

(Received 26 July 1993)

We present examples of simple dynamical systems containing alternative routes to chaos which are degenerate with a period-doubling route. The existence of degenerate routes implies the possibility of having more entangled dynamical behaviors hidden in observations based on a single-variable time series, possibly requiring, therefore, special care to discriminate them. A model system allowing the investigation of transitions between degenerate routes is also considered.

PACS number(s): 05.45.+b, 02.30.-f, 02.90.+p

Period doubling is well known for providing in dissipative systems a route from regular to chaotic behavior which is known to have *universal* properties [1]. This route has been described in several books; for example, in Refs. [2–5]. Period-doubling routes to chaos have been shown to exist both in measurements and models of phenomena observed in virtually all branches of the natural sciences. Such routes are presently known to be robust characteristics found in mathematical models of natural phenomena, independently of whether these models involve partial differential equations, systems of ordinary differential equations, difference-differential equations or just “simple” discrete maps. Textbook examples of discrete mappings are the one-dimensional *quadratic* map

$$x_{t+1} = a - x_t^2, \quad (1)$$

a simpler normal form of the logistic equation [1–5], and a two-dimensional map closely related to it, the Hénon map [6],

$$x_{t+1} = a - x_t^2 + by_t, \quad (2a)$$

$$y_{t+1} = x_t. \quad (2b)$$

For  $b=0$ ,  $x_t$  and  $y_t$  in Eq. (2) are independent variables and measurements of any of them will always reflect the one-dimensional characteristics of Eq. (1) rather than any two-dimensional aspects. But if  $b \neq 0$ , how far from zero must it be to ensure the possibility of recognizing with confidence that the variables are interdependent? A non-trivial question seems then to be whether, based solely on a single-variable time series, it is still possible to recover the dimensionality of the system in this adverse situation, i.e., for  $b \neq 0$  but small, to recognize which of the dynamic systems, the one-dimensional Eq. (1) or the two-dimensional Eq. (2), is generating the series. This question is equivalent to quantifying how small might parameters be before we lose the ability to recognize interdependency between variables. The analysis of single-variable time series and the reconstruction of the corresponding phase-space is presently a subject of enormous activity. An idea of the current status of the field might be obtained by perusing the many papers and references

contained in 500 pages of the proceedings of a recent symposium [7]. At first, it might perhaps appear that the slaving implied by the equation of motion  $y_{t+1} = x_t$  is too simple to be of any use. Quite to the contrary, this equation implies the existence of an important degeneracy between return maps and attractors. It is not difficult to construct a variety of interesting situations where one or several variables are forced to follow the others closely. Recent work [8] has shown how to generate and interpret a whole hierarchy of non-Markovian processes based on the entanglings implied by equations such as  $y_{t+1} = x_t$ . In this paper we would like to discuss the consequences of an interesting particular class of processes, namely, compositions of  $x_{t+1} = a - x_t^2 - \tau$ . We believe such processes to be of help in analyzing and understanding single-variable time series obtained from multidimensional dynamical systems, either in the laboratory or with computers.

This paper presents models that show that period-doubling routes to chaos observed in multidimensional systems might be sometimes *degenerate with other bifurcation routes*. While mathematical models of physical phenomena invariably assume an *a priori* knowledge of the number of variables responsible for the dynamics, experimentally it is frequently not trivial to obtain such information. In fact, a fundamental quantity sought in experiments is exactly the underlying *dimensionality* of the system. This dimensionality is commonly extracted from the analysis of single-variable time series through relatively sophisticated *embedding techniques* [2–5,7] used to reconstruct the phase space. The models considered in this paper show that single scalar time series may subtly hide more complicated dynamical behaviors that might easily go unnoticed if one is not paying explicit attention to them. The most general model considered here is that defined in Eq. (5) below. We start by first considering a particular limit of it, Eq. (4), presenting then the general model. Of particular interest is an investigation of how transitions from one route to others occur. The models proposed here are admittedly simple. However, they are not more artificial than any of the aforementioned models, models proven to be quite reliable [1–5] in describing and anticipating phenomena found in real life.

Identical figures are obtained if one considers either  $x_t \times a$  or  $y_t \times a$  bifurcation diagrams for the following trivial two-dimensional *embedding* of the quadratic map:

$$x_{t+1} = a - x_t^2, \tag{3a}$$

$$y_{t+1} = x_t. \tag{3b}$$

This embedding coincides with the uncoupled  $b = 0$  limit of the Hénon map, Eq. (2), in which  $y_t$  is slaved to follow  $x_t$  forever. Consider now the following alternative model:

$$x_{t+1} = a - y_t^2, \tag{4a}$$

$$y_{t+1} = x_t, \tag{4b}$$

the basic building block for an infinite hierarchy of processes [8]. In Eq. (4),  $x_t$  and  $y_t$  are parametrically coupled and it is not totally trivial to anticipate the dynamics to be expected from it. It is possible, however, to verify numerically that both bifurcation diagrams,  $x_t \times a$  and  $y_t \times a$ , in this case also perfectly overlap each other and, further, that they perfectly overlap with bifurcation diagrams corresponding to Eq. (1). In other words, all these bifurcation diagrams represent in fact a *fourfold degenerate* diagram: two corresponding to the variables of Eq. (3) and another two corresponding to those of Eq. (4). Do these identical diagrams contain something new or are they simply repeating information already known? Figure 1 presents “generalized bifurcation trees” in the  $(x_t, y_t, a)$  space, along with corresponding projections of the trees on the  $x_t \times y_t$  planes. As seen from the figure, while the embedded quadratic map follows the familiar  $1 \rightarrow 2 \rightarrow 4 \rightarrow 8 \rightarrow \dots$  doubling route to chaos, the map of Eq. (4) is seen to follow a new “shifted”  $1 \rightarrow 4 \rightarrow 8 \rightarrow 16 \rightarrow \dots$  route. Figure 1 shows that although the bifurcation trees of Eqs. (3) and (4) have iden-

tical projections on the planes  $x_t \times a$  and  $y_t \times a$ , with corresponding bifurcations occurring at exactly the same values in parameter space, both models in fact display *quite different* dynamics and routes to chaos in phase space. Accordingly, the route to chaos of Eq. (4) has several scaling properties identical to those from the familiar doubling route [1]. Since 1978, the period-doubling route of Eq. (3) has been extensively investigated both theoretically and experimentally. However, the possibility of having routes to chaos *degenerated* with the period-doubling route does not seem to have been noticed before. Other types of degenerate routes may be obtained by considering compositions other than quadratic and for systems with larger dimensions.

How are *transitions* between degenerate routes expected to occur in physical systems in general? To address this question we combine Eqs. (3) and (4) *ad hoc* into the following dynamical system:

$$x_{t+1} = a - py_t^2 - qx_t^2, \tag{5a}$$

$$y_{t+1} = x_t. \tag{5b}$$

The additional parameters  $p$  and  $q$  are introduced to allow convenient *tuning* the relative influence of the term they control, in particular, to go from Eq. (5) to either Eq. (3) or (4). Figure 2 shows *isoperiodic diagrams* [9], i.e., diagrams in parameter space displaying regions of similar periodicity for two cuts of the parameter space of Eq. (5). Figure 2(a) was obtained maintaining  $p = 1$  and varying  $a$  and  $q$ , while in Fig. 2(b) we kept  $q = 1$  and let  $a$  and  $p$  vary. The horizontal (vertical) axis was discretized into 1024 (768) equally spaced intervals. In both figures, similar shadings are used to represent similar asymptotic periodicities found for Eq. (5). The shading of the large region containing the symbol  $\infty$  corresponds to parameters for which generic initial conditions lead to unbounded orbits. White regions correspond to chaos, i.e., to parameters for which the dynamics does not diverge after 5000 iterates and, within the precision of the calculations, is also not found to have subsequently any numerically detectable periodicity. The large black region corresponds to parameters leading to fixed points. This region contains interesting borders: a  $D$  border, across which one finds the usual  $2^n$  doubling route to chaos, and a  $C$  border along which, as the figure shows, very complex dynamics exists. Following horizontal lines across the  $D$  border one eventually reaches the limit set where  $1 \times 2^n$  standard doubling cascades accumulate. This limit set is indicated by the symbol  $2^\infty$  in the figures. Other shadings correspond to regions of different periodicity, with integers always indicating the main periodicity after period 1. As  $a$  increases in Fig. 2, the several adjacent regions to the right of the period 3, 4, 5, etc. correspond respectively to full doubling cascades of these periods. There is an infinite but perfectly countable sequence of isoperiodic regions having main periodicities  $k$  ( $k$  an arbitrary integer), which are born at the  $C$  border. The symbols  $S_i$  are used to indicate regions where there is a particularly high concentration of isoperiodic structures somewhat similar to the shrimps discussed in Refs. [9] and [11] and starting with virtually any integer period  $k$ .

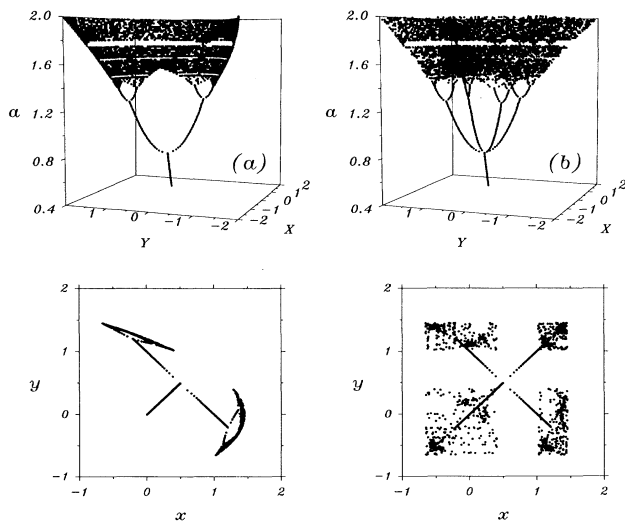


FIG. 1. Generalized bifurcation trees “removing” the degeneracy: (a) the two-dimensional embedding of the quadratic map [Eq. (3)], and (b) the alternative map of Eq. (4). Below each tree one sees the corresponding two-dimensional projections on the  $x_t \times y_t$  plane.

The *C* and *D* borders meet at a “triplex” point, which belongs simultaneously to the border of three different regions. Along *C* the dynamics is complex and indeed very reminiscent of that known for *conservative* systems. The fact that the Jacobian,  $J=2py_i$ , of Eq. (5) depends on  $y_i$  makes the characterization of Hamiltonian regimes a nontrivial task here. From Fig. 2(b) one sees that adding a low-amplitude  $y_i^2$  term to the “dominant”  $x_i^2$  does not change the dynamics close to the line  $p=0$  significantly. In contrast, as seen from Fig. 2(a), adding  $x_i^2$  perturbations to  $y_i^2$  produces most of the time rather drastic changes. Figure 2(a) also shows that by properly choosing specific constant values for  $q$  (in addition to maintaining  $p=1$ ) it is possible to generate an infinite number of new routes to chaos. These new routes are characterized by having regions of any integer periodicity (plus corresponding cascades) following the basic period-1 region. For example, for  $p=1$  and  $q=0$  one finds the particular shifted route displayed in Fig. 1.

Why do both limits of Eq. (5) display nonhyperbolic behavior at exactly the same values of  $a$ ? The stability of period-1 solutions of Eq. (5) is determined by the magnitude of the eigenvalues of the fixed points  $(x_+, x_+)$  and  $(x_-, x_-)$ , defined by  $2(p+q)x_{\pm} = -1 \pm [1+4a(p$

$+q)]^{1/2}$ . Real fixed points exist as soon as  $a \geq -1/[4(p+q)]$ . This shows that the actual location of fixed points depends only on  $p+q$ , and not on their individual values. The eigenvalues of a generic point  $(x, y)$  are  $-qx \pm [(qx)^2 - 2py]^{1/2}$ , and, accordingly, the stability of  $x_+$  and  $x_-$  is respectively determined by  $\Lambda_{\pm}(a, p, q) = -qx_{\pm} \pm [q^2x_{\pm}^2 - 2px_{\pm}]^{1/2}$  and  $\lambda_{\pm}(a, p, q) = -qx_{\pm} \pm [q^2x_{\pm}^2 - 2px_{\pm}]^{1/2}$ . For the cases of main interest here one has explicitly

$$\Lambda_{\pm}(a, 1, 0) = \pm \sqrt{-2x_{\pm}}, \tag{6a}$$

$$\lambda_{\pm}(a, 1, 0) = \pm \sqrt{-2x_{\mp}}, \tag{6b}$$

and

$$\Lambda_{\pm}(a, 0, 1) = -x_{\pm} \pm |x_{\pm}|, \tag{7a}$$

$$\lambda_{\pm}(a, 0, 1) = -x_{\mp} \pm |x_{\mp}|. \tag{7b}$$

Since for both equations one has  $p+q=1$ , in both cases fixed points are defined by  $2x_{\pm} = -1 \pm \sqrt{1+4a}$ . These eigenvalues are plotted in Fig. 3 as functions of  $a$ . Stable orbits are guaranteed when the magnitude of both eigenvalues is not larger than unity. Due to the peculiar dependence of Eqs. (6) and (7) on  $p, q$ , and  $a$ , the *range of*

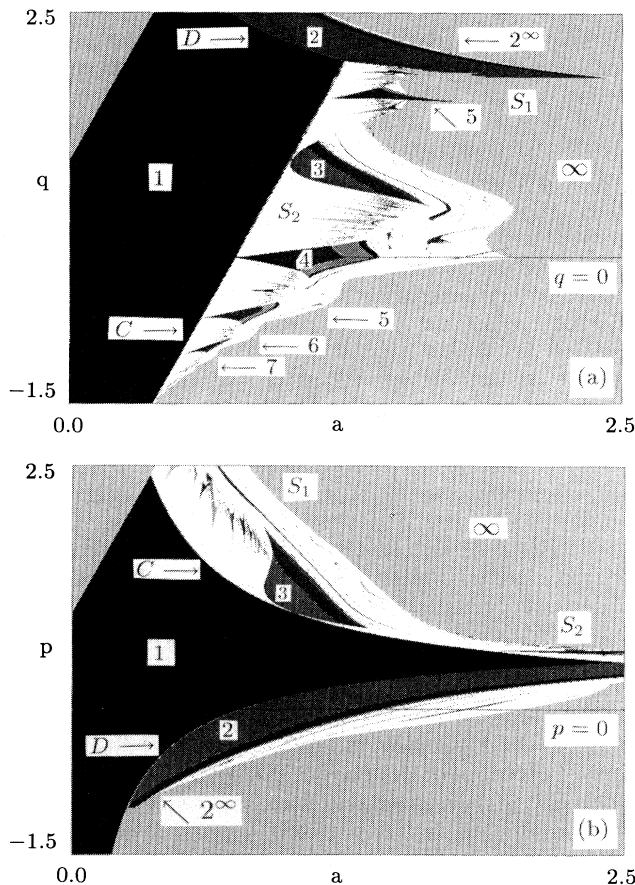


FIG. 2. Isoperiodic diagrams showing transitions between degenerate routes for two cuts of the parameter space of Eq. (5). (a)  $p=1$ ; (b)  $q=1$ . Horizontal lines mark the limiting cases of Eqs. (4) and (3), respectively.

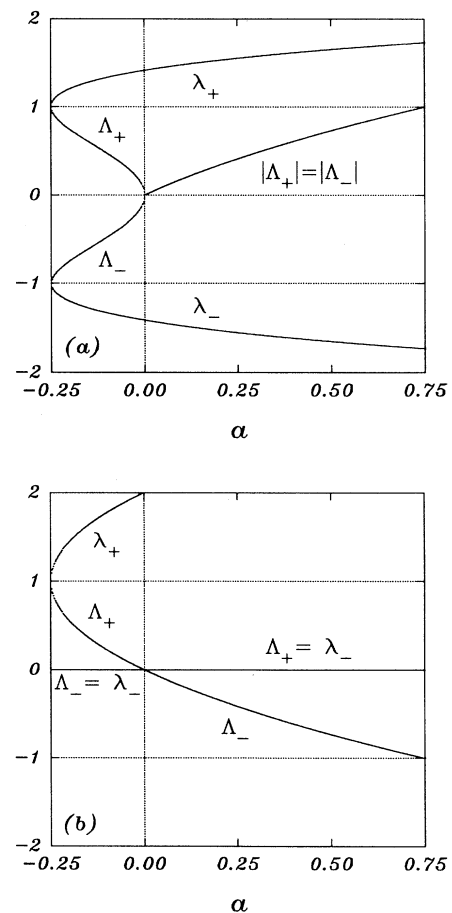


FIG. 3. Eigenvalues for two limits of Eq. (5): (a) Eq. (6), corresponding to the alternative map in Eq. (4); (b) Eq. (7), the embedded quadratic map in Eq. (3).

stability of the fixed points for the new map of Eq. (4) coincides with that of the embedded quadratic map, Eq. (3). A major difference is that while Eq. (3) always has real eigenvalues, Eq. (4) has a pair of pure imaginary eigenvalues for  $a > 0$ . In this case Fig. 3 gives the absolute value of the eigenvalues. As seen from Fig. 3, while  $x_+$  is always a stable attracting fixed point for both models,  $x_-$  changes from the familiar saddle node to a repeller.

Comparison between both  $x_t \times y_t$  projections in Fig. 1 shows that, in addition to a different route to chaos, one might also anticipate rather different characteristics to be present in the chaotic regime of both models. In Fig. 1, both  $x_t \times y_t$  projections are for  $0 \leq a \leq 1.45$ , i.e., for parameter values before the characteristic tangency where nonconnected chaotic bands osculate each other. Further, rather than plotting many points  $(x_t, y_t)$  after a convenient number of preiterates, just a few of them were given in order to allow the several branches of the generalized bifurcation tree to be seen. This also permits us to have a rough idea of the statistical distribution of points on the  $x_t \times y_t$  plane at  $a = 1.45$ . Plotting more points would simply ergodically fill the four rectangles already discernible in Fig. 1. While all chaotic attractors of Eq. (3) have geometric shapes that in spite of being one dimensional are relatively complicated to write down analytically, chaotic attractors for Eqs. (4) and (5) are extremely well behaved geometrically, being always composed of one or several rectangles. For higher values of  $a$ , the attractor is a single square. Basins of attraction also display the same simple geometric structure. These aspects are of theoretical interest in investigating the intertwining of manifolds to locate analytically interesting homoclinic and heteroclinic tangencies, to test the reliability of some "chaos-indicator" criteria, and to characterize ergodic properties. For example, for  $a = 2$  and generic initial conditions, it can be shown that the basin of attraction and the attractor itself coincide both with one and the same square. Even simpler chaotic attractors exist for some particular initial conditions. All these properties seem to point to the possibility of finding with reduced labor rigorous proofs for aspects of the dynamics of high-dimensional systems such as that in Eq. (5). Therefore the model in Eq. (5) and its variants might also be of some interest for mathematicians. The behavior be-

ing reported to exist beyond the  $C$  border is that already familiar from systems displaying quasiperiodicity. A study of quasiperiodicity generated by Eq. (5) and similar ones (which display intrinsic quasiperiodicity arising from the interplay of variables and/or parameters, not one from toroidal phase spaces created somewhat artificially by congruences) along with a discussion of a general real quadratic mapping of the plane on the plane will be presented elsewhere [10].

We conclude by noting that degenerate routes to chaos as reported here were also seen [11] in a few more complex situations and, therefore, are not believed to simply represent nongeneric pathologies. As further examples we mention briefly the system represented by

$$x_{t+1} = a - y_t^2, \quad (8a)$$

$$y_{t+1} = b - x_t^2, \quad (8b)$$

and the system

$$x_{t+1} = (a - x_t^2)^2 - b. \quad (9)$$

Apart from displaying the same route degeneracy in phase space as Eqs. (3) and (4), these two systems were shown [11] to have all borders of stability totally degenerate in parameter space. Quadratic compositions in higher dimensions generate an arbitrary number of different routes to chaos in phase space which may be suitably combined to produce common borders of stability in parameter space. For example,  $(x, y, z) \mapsto (a - z^2, b - x^2, y)$  produces a  $1 \rightarrow 6 \rightarrow 12 \rightarrow \dots$  route in phase space, but a subdivision of the parameter space that coincides with that obtained from either Eq. (8) or (9). Different and interesting classes of degenerate routes worth investigating arise from mixed compositions, i.e., from compositions which do not necessarily involve only quadratic dynamics, or else which involve only dynamics higher than quadratic.

The author thanks the University of Maryland and the Forschungszentrum Jülich for their hospitality. He thanks Professor C. Grebogi, Professor H. J. Herrmann, and Professor J. A. Yorke for their kind hospitality and for many stimulating discussions.

- 
- [1] M. J. Feigenbaum, *J. Stat. Phys.* **19**, 25 (1978); **21**, 669 (1979).  
 [2] H.-O. Peitgen, H. Jürgens, and D. Saupe, *Chaos and Fractals, New Frontiers of Science* (Springer, New York, 1992).  
 [3] A. J. Lichtenberg and M. A. Lieberman, *Regular and Chaotic Dynamics*, 2nd ed. (Springer, New York, 1992).  
 [4] P. Manneville, *Dissipative Structures and Weak Turbulence* (Academic, Boston, 1990).  
 [5] J. Guckenheimer and P. Holmes, *Nonlinear Oscillations, Dynamical Systems, and Bifurcations of Vector Fields* (Springer, New York, 1983), corrected third printing.  
 [6] M. Hénon, *Comm. Math. Phys.* **50**, 69 (1976).  
 [7] *Interpretation of Time Series from Nonlinear Systems*, in Proceedings of the International Union of Theoretical and

- Applied Mechanics Symposium and NATO Advanced Research Workshop, Warwick [Physica D **58**, 1 (1992)].  
 [8] J. A. C. Gallas, *Physica A* **195**, 417 (1993); **198**, 339(E) (1993).  
 [9] J. A. C. Gallas, *Int. J. Mod. Phys. C* **3**, 1295 (1992); *Phys. Rev. Lett.* **70**, 2714 (1993); F. Cabral, A. Lago, and J. A. C. Gallas, *Int. J. Mod. Phys. C* **4**, 553 (1993); J. A. C. Gallas, C. Grebogi, and J. A. Yorke, *Phys. Rev. Lett.* **71**, 1359 (1993).  
 [10] J. A. C. Gallas (unpublished).  
 [11] J. A. C. Gallas, *Höchstleistungsrechenzentrum Report No. HLRZ 48/93* (1993) (unpublished); *Physica A* (to be published).